Title
MICROSTRUCTURAL BASIS OF ALLOY DESIGN FOR HIGH STRENGTH, TOUGH STRUCTURAL STEELS

Author
Thomas, G.

Publication Date
1981-09-01

Lawrence Berkeley Laboratory

UNIVERSITY OF CALIFORNIA

Materials & Molecular Research Division

Presented at The Metals Society Advances in Physical Metallurgy and Applications of Steels Conference, Liverpool, United Kingdom, September 21-24, 1981

MICROSTRUCTURAL BASIS OF ALLOY DESIGN FOR HIGH STRENGTH, TOUGH STRUCTURAL STEELS

G. Thomas, M. Sarikaya, G.D.W. Smith, and S.J. Barnard

September 1981

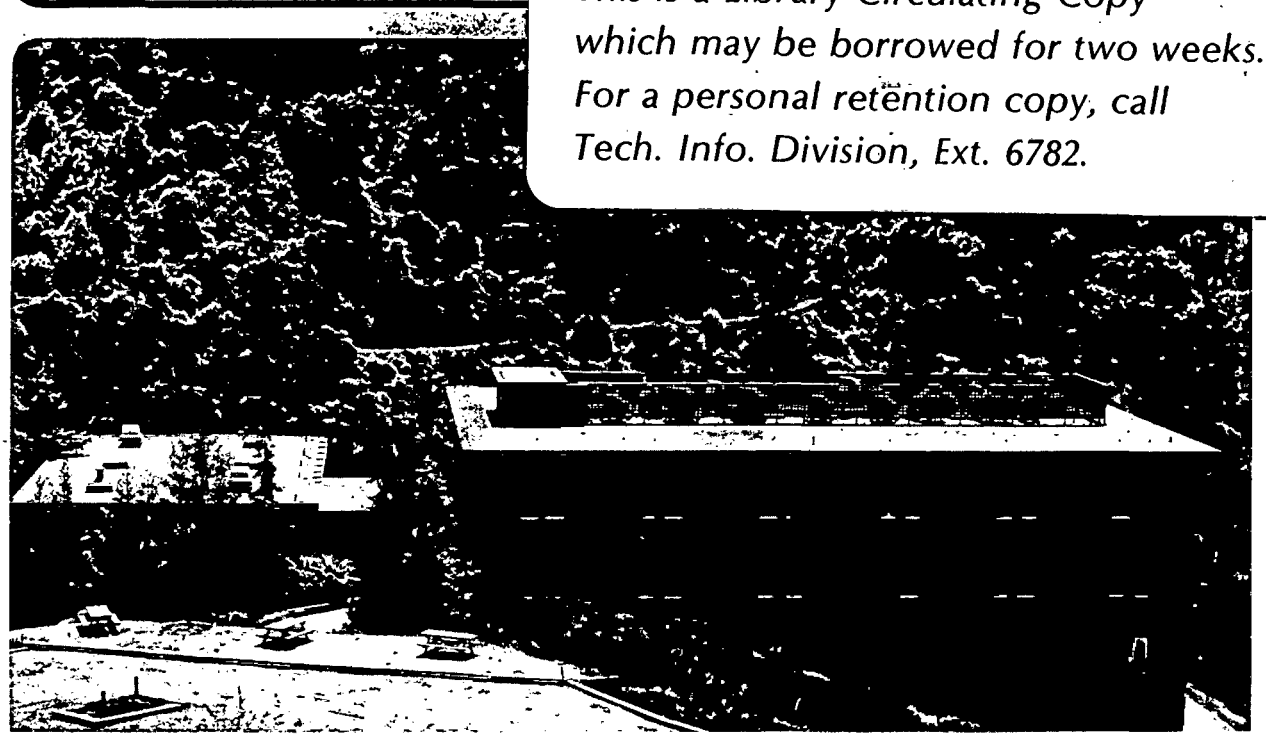

Prepared for the U.S. Department of Energy under Contract DE-AC03-76SF00098

DISCLAIMER

MICROSTRUCTURAL BASIS OF ALLOY DESIGN FOR HIGH STRENGTH, TOUGH STRUCTURAL STEELS*

G. Thomas[1], M. Sarikaya[1], G. D. W. Smith[2], and S. J. Barnard[2]

Abstract

Optimum mechanical properties may be obtained in medium carbon steels with microstructures consisting of dislocated lath martensites in which laths are surrounded by films of retained austenite. Direct studies of the chemical composition of the retained austenite phase, using the experimental technique of atom probe microanalysis, show that the austenite is substantially enriched in carbon and a large peak in carbon concentration is found at the austenite/martensite interface even in the as-quenched condition. Carbon partitioning depleting the martensite matrix must occur during transformation. Although the enrichment of austenite by carbon provides some chemical stability, mechanical stabilization must also be a major factor. The austenite may be destabilized by tempering or by plastic deformation. The relationship between these results and the strength and fracture toughness properties of a range of Fe-Cr-0.3C steels containing Mn or Ni are presented, together with recent results of in situ studies of fracture in a high voltage electron microscope.

---

1) Department of Materials Science and Mineral Engineering, University of California, Lawrence Berkeley Laboratory, Berkeley, CA 94720.

2) Department of Metallurgy and Science of Materials, University of Oxford, OX1 3PH (U. K.).

A. Introduction

High strength structural steels are used extensively for components such as aircraft landing gear, missiles, rocket casings, armour plate, and other defence applications. In addition, where such steels have high hardness and consequent abrasion resistance, they are used in mining operations (for example, as buckets and in communution and mineral processing operations). The limiting factor in the use of high strength steels is their toughness. In practice, toughnes and ductility are required to resist crack propagation and ensure sufficient formability for successful fabrication of the steel into engineering components. Many commercial high strength steels in use today have been designed by experience, often by trial and error, and almost all of those at high strength levels could benefit from improvements in toughness.

With this objective in mind, a systematic study of the relation between martensitic microstructures and properties utilizing a series of Fe-C-X high purity, vacuum melted experimental steels (where X is the substitutional solute) has been under way at Berkeley for over 15 years (e.g., see Refs. 1,2 for review). The martensite transformation, if controlled so that the inhomogeneous shear component occurs by slip and not by twinning, is the most efficient means of producing dense, uniformly dislocated fine grained structures.[3] The dislocations are an essential component for strength and toughness. The main factor controlling this aspect of the transformation is composition, especially carbon content (affecting transformation temperature M_s and strength of martensite), which must be regulated to maintain $M_s > 200°C$. This sets the carbon limit to about 0-3%. As a result of detailed analyses by electron

microscopy and diffraction, austenite was detected, although its presence was not expected. In addition, it has been found that this retained austenite, if stable, promotes toughness.[1-3] Consequently, the microstructure which corresponds to optimum mechanical properties is a duplex austenite-martensite structure in which packets of laths are surrounded by austenite films, shown schematically in Fig. 1, and an actual example is given in Fig. 2. Since each packet corresponds to laths of a particular $(111)_\gamma$ variant, the maximum number of variants in a prior austenite grain is four, although several packets of the same variant can be present. These packets thus serve to refine the microstructure. The excellent combinations of strength and toughness exhibited by the steels so developed, even in the untempered condition, can be seen in Fig. 3.

Of course, tempering the 300°-400°C range leads to tempered martensite embrittlement associated with decomposition of the retained austenite to interlath carbides.[3] The microstructures and fractographic changes are shown in Feg. 4 which compares the in situ and ex-situ fracture characteristics.

Recently, new data[5,6] have been obtained on the carbon and substitutional atom distributions in these duplex steels. Although the terminology "lath martensite" will still be retained, it is emphasized that perhaps the terminology "untransformed upper bainite"[4] would be better. This viewpoint is confirmed by the microanalytic results to be summarized here. The main points we wish to emphasize in this paper are:

1. The partitioning of carbon between martensite, retained austenite, and the interfaces between them.
2. The stability of retained austenite.
3. The relation between microstructure and fracture toughness.

B. Experimental

Alloys Investigated

A wide range of alloys has been developed over the years especially to study individually the role of C, Cr, Mn, Ni, Mo, etc. and details may be found in the literature (e.g. Ref. 1). Typical compositions of the most recently developed alloys are given in Table 1, in which air melted and vacuum melted steels have been studied. All steels are austenitized at 1100°C to dissolve all carbides, oil quenched and tempered. Table 2 shows typical properties of the vacuum melted steels.

Metallography

Specimens from bulk samples were prepared in the usual way for transmission electron microscopy/scanning transmission electron microscopy (TEM/STEM) observations[1] (Fig. 2) and wires prepared for the FIM atom probe studies.[3] In addition, thin foils so prepared were also examined under in situ deformation conditions in the AEI 1 MeV microscope at the Max-Planck Institut Stuttgart, so as to directly observe the fracture process. Fractographic analysis of broken bulk specimens was performed by scanning electron microscopy.

C. Results

Microstructure and microanalysis

The microstructural and crystallographic details of these steels are now well documented,[1-4] and it is necessary here only to show typical examples (Figs. 2,3a,b). However, little information on local composition and its distribution throughout the microstructure (Fig. 2) was obtained until the new techniques of high resolution electron microscopy, diffraction, especially convergent beam electron diffraction,

and spectroscopy and field ion-atom probe spectroscopy became available. Details of such investigations are published elsewhere,[4-6] and the main findings are summarized as follows:

1. Lattice imaging[4] indicated indirectly that the carbon content in austenite could be as high as ∿3 at. %.
2. Convergent beam microdiffraction[6] verified this first result.
3. More convincingly, atom probe spectroscopy not only verified the indirect lattice parameter measurements but also, uniquely, gave information on the carbon content at the austenite/martensite interface.[3,6]

Typical atom probe data are shown in Figs. 5a,b and 6a and in Table 3. These results show that this distribution of carbon does not change very much between the as-quenched (quench rate up to 10^3K s^{-1}) and the 200°C tempered conditions.[6] Thus, carbon redistribution must occur during transformation,[6] i.e., at and below Ms. Since the M_s temperature for these steels is about 300°C or above, there is adequate time for carbon diffusion to occur. The particular importance of this result on austenite stability[6] and mechanism of the transformation[4,9] is discussed elsewhere.

Microstructure and Fracture

Metallography and fracture: These medium carbon steels are very tough in the as-quenched condition, but the Charpy and K_{1C} toughness values improve with 200°C tempering (Table 2). It should also be noted that the toughness and tensile ductilities do not correlate very well, e.g., the tensile ductility is 7% for both the 200°C and 500°C tempered conditions, yet the respective Charpy values are 47 and 27 N-M.

The gain in toughness after 1 h tempering at 200°C is almost certainly due to relief of internal strains associated with local redistribution of carbon within the laths. Figure 6a shows a high carbon peak at the martensite/austenite interface. This peak is higher and broader than that seen in the as-quenched alloys (Fig. 5b). In both cases, electron microscopy shows retained austenite to be the interlath phase with no evidence for carbides at the interface (Figs. 2 and 6b). The atom probe data must therefore indicate pre-precipitate clustering of carbon-rich regions. Current research on isothermal aging shows that the volume fraction of the retained austenite decreases before carbides have been detected in the microstructure. When retained austenite is replaced by carbide (Fig. 4b), embrittlement occurs as indicated by the decrease in Charpy values (Table 2). Presumably, the retained austenite decomposes as a result of interfacial precipitation and growth of the carbide phase. Detailed analyses of these tempering processes are now being studied.

In an attempt to resolve directly the possible effects of retained austenite on the increased toughness, in-situ experiments have been performed whereby thin foils of quenched and quenched and tempered steels corresponding to those listed in Table I have been strained until fracture in a high voltage electron microscope. Typical examples compared to conventional fractography are shown in Fig. 4. While it is realized that deformation of foils of thickness of the order of a few thousand angstroms is not directly comparable to bulk data, e.g., from a K_{1C} test (deformation in thin foil approximates plane stress conditions while that in a K_{1C} test reflects plane strain conditions), the results suggest some ideas which are outlined in the following:

1. Fracture always takes place in the martensite laths with cracks running parallel to the lath axes normal to the tensile stress (Fig. 4a,b).

2. In the tough condition, fracture is preceeded by slip, i.e., dislocation motion and local thinning - necking (as in a bulk tensile test), void formation and coalescence. This can occur across parallel laths in the packet. An idea of the strain distribution in the packet can be seen in Fig. 4a.

3. The overall microstructure affects the slip distribution and hence the plasticity of the martensite.*

Thus in steels tempered to the embrittled condition (TME), the interlath austenite transforms to cementite and slip is then confined to a particular lath. Metallographically the situation is rather like intergranular fracture in age-hardened alloys where the slip distribution is determined by the grain boundary precipitation morphology.[10] The fracture path is then transgranular (Fig. 4b) with respect to prior austenite, and by comparison to Fig. 4d shows that this is consistent with fracture inside and along the laths themselves. This suggests that the plastic zone is confined to single laths.

Qualitatively, the in situ fracture observations, mechanical properties and fractography correlate reasonably well. For tough alloys, the plastic zone ρ must be quite large. The plastic zone size is given by fracture mechanics as:

---

*A film of this process has been made (contact G. Thomas for details) The tensile stage used does not allow measurements to be made of the stress, strain or strain rate.

$$\rho = \frac{1}{6\pi} \left[\frac{K_{1C}}{\sigma}\right]^2$$

and the choice of σ value is important. In ductile steels, σ must be close to the tensile strength since crack growth is associated with local necking in parallel laths, void formation and cross-linking of these regions.* Hence, the plastic zone size corresponds roughly to the packet size (20-50 μm) of those laths favourably oriented for deformation under the applied stress. One would then expect a dimpled fracture of dimple size roughly equal to the packet size. This is seen in Fig. 4c. In Fig. 4a, the strain contrast surrounding the crack indicateds a strain zone of about 20 μm, which is consistent with the above discussion.

On the other hand, in the TME condition the interlath carbides restrict slip to the laths themselves. Strain zones such as those visible in Fig. 4a do not appear (Fig 4b). Thus, the plastic deformation is contained within a given lath. This implies that the minimum plastic zone size is the lath width, which is of the order of 1 μm. From the above equation, for ρ = ultimate tensile strength (UTS), the K_{1C} value would be very small (8 MPa $m^{-\frac{1}{2}}$).

As fracture proceeds down a particular lath, it zig-zags along the {110} slip plane projections leading to long cracks with little or no coalescence across the packet (Fig. 4b). This process is also confined to {110} paths due to the {110} interlath carbides. The crack is confined to a particular lath by the bounding interlath carbide film and cannot cross over to an adjacent lath until there is no carbide barrier. This can be seen in Fig. 4b. The fractograph then expected would show elongated patterns corresponding to the orientations of laths in a

packet, namely, transgranular with respect to prior austenite. Fracture thus proceeds by continued crack propagation along the laths. This picture is consistent with the fractographic observations (e.g. Fig. 4d).

Retained austenite: No direct evidence has so far been obtained which uniquely identifies why the interlath films of austenite appear to improve toughness (Fig. 3). Many suggestions have been discussed previously,[1] including transformation of austenite under stress. Bulk observations of fractured surfaces by Mössbauer spectroscopy at Berkeley indicate that austenite has transformed in this region. Electron microscopy shows some evidence of twinned martensite near the fracture in thin foils.[11] Since the carbon content of the retained austenite can be as high as 3 at. %, any martensite transformation of this austenite would lead to twinned martensite, but the crystallography is not the same as that for the original martensite laths in a packet. This point will be discussed in more detail elsewhere.[11] These observations are in agreement with those reported by Eterashvili and Utevsky.[12] However, the in-situ studies show that austenite does not always transform, i.e. a crack growing through a lath may still be surrounded by untransformed austenite. Of course, the stress conditions in a foil may not be favorable (CRSS to transform austenite) and the austenite, already thin in lateral dimension (50-100Å), is also thin in the thickness direction of the foil (∿1000Å) and so the size effect may also be a factor (it is well known that below certain sizes, depending on composition, particles of austenite resist transformations, e.g. Ref. 13).

Martensite: Another consequence of the carbon partitioning during transformation is that the carbon content of the laths is decreased by about 10% of that of the nominal composition of the alloy in regions adjacent to the austenite (Fig. 6). This value is indirectly estimated from the atom probe analysis. Since the strength of dislocated martensite is linearly proportional to the carbon content, a lower carbon martensite will be "softer" and more ductile. The in situ fracture experiments show that fracture in martensite is preceded by extensive local slip and necking down ; i.e. fracture occurs following local work hardening. So it may be that the presence of austenite indirectly favours such processes in the laths. Since the dislocation density is very high ($\sim 10^{12}/cm^2$) in martensite after the transformation, unpinned dislocations are needed for slip and work hardening. Also, the austenite/martensite interface is semi-coherent, with good matching between the (110) slip planes in martensite and the (111) planes in austenite,[4] and slip can thus transfer relatively easily across the martensite/austenite interface; i.e. interlath austenite does not restrict slip within a single martensite lath. On the contrary, as we have seen above, when the austenite is tempered to decompose into interlath carbide, slip is then confined to the lath interior.

D. Conclusion

A general conclusion, then, is that the fracture characteristics of low and medium carbon steels are determined by the plasticity of martensite, which in turn is, of course, determined by the microstructural effects on slip within the laths and the compositional changes (especially

carbon) associated with the presence of retained austenite. From an alloy design viewpoint, it is thus essential to obtain dislocated laths and this is why control of composition and heat treatment is vital.

Acknowledgements

The Berkeley alloy design programme is supported by the Director, Office of Energy Research, Office of Basic Energy Sciences, Materials Sciences Division of the U. S. Department of Energy under Contract No. DE-AC03-76SF00098. One of the authors (G.T.) acknowledges the Humboldt Senior Science award which allowed in situ experiments to be carried out at the Max-Plank Institute, Stuttgart. The assistance of Dr. M. Rühle and his staff in this work is much appreciated. S. J. B. and G. D. W. S. acknowledge the financial support of the U. K. Science Research Council and the provision of laboratory facilties by Professor Sir P. B. Hirsch, FRS. The science scholarship by TUBITAK-BAYG (Turkey) is also acknowledged (M.S.).

References

1. B. V. N. Rao and G. Thomas, Met. Trans. A11, 441 (1980).

2. G. Thomas, Ibid. A9, 439 (1978).

3. G. Thomas in Fundamental Aspects of Structural Alloy Design, R. I. Jaffee and B. A. Wilcox (Eds.), Plenum Press, N. Y., 1977, p. 331.

4. B. V. N. Rao and G. Thomas, ICOMAT Conference, M. I. T. Press, 1979, p. 12. Also Ref. 9.

5. S. J. Barnard, G. D. W. Smith, M. Sarikaya and G. Thomas, Scripta Metallurgica 15, 387 (1981).

6. M. Sarikaya, G. Thomas, J. W. Steeds, S. J. Barnard and G. D. W. Smith, Int. Conf. on Phase Transformations, Pittsburgh 1981 (ASM, in press).

7. M. Sarikaya, B. G. Steinberg and G. Thomas, Met. Trans. 1981 (to be published in December 1982 issue.)

8. G. Thomas, to be published.

9. G. Thomas and M. Sarikaya, Int. Conf. on Phase Transformations, Pittsburgh 1981 (ASM, in press).

10. G. Thomas and J. Nutting, J. Inst. Metals 87, 429 (1959).

11. M. Sarikaya, J. W. Steeds and G. Thomas (to be published).

12. T. V. Eterashvili and L. M. Utevsky, Eurem 1980 i, 184 (Netherlands Society for Electron Microscopy).

13. K. E. Easterling and R. R. Swann, Acta Met. 15, 117, (1971).

TABLE II MECHANICAL PROPERTIES OF VACUUM MELTED SINGLE TREATED STEELS

Alloys**	T tempering temperature, °C	Hardness HRC	0 2% Offset YS ksi	YS MPa	UTS ksi	UTS MPa	% Elongation Total (uniform)	K_{1C} ksi $in^{-\frac{1}{2}}$	K_{1C} MPa $m^{-\frac{1}{2}}$	Charpy V-notch Energy ft lb	Charpy V-notch Energy N-m
V1	AQ	49	200	1378	253	1743	6.3(3.5)	80.0	89.0	28.7	39.0
	200	48	205	1413	257	1771	7.1(2.6)	110.5	123.0	34.5	46.8
	300	45	177	1220	206	1419	8.0(2.8)	---	---	22.5	30.5
	400	42	170	1171	200	1378	8.1(2.7)	---	---	22.0	30.0
	500	41	166	1144	194	1337	7.0(3.7)	---	---	20.0	27.0
	600	35	126	868	144	992	14.6(4.5)	---	---	50.3	68.0
V2	AQ	50	197	1357	255	1757	8.1(3.3)	77.7	86.0	31.4	42.5
	200	48	199	1368	248	1709	8.9(3.2)	100.0	111.0	35.3	48.0
	300	44	173	1192	206	1419	9.4(2.4)	---	---	28.5	39.0
	400	43	167	1151	194	1337	10.5(2.6)	---	---	27.0	36.5
	500	40	160	1102	187	1281	12.2(3.1)	---	---	35.5	48.0
	600	36	129	885	146	1002	16.8(5.2)	---	---	90.3	122.5

TABLE I

ALLOY COMPOSITIONS AND TRANSFORMATION TEMPERATURES

Alloy	Composition, wt-%											Temperature, °C			
	Cr	C*	Mn	Ni	Mo	Si	Cu	Al	P	S	Fe	M_s	M_f	A_s	A_f
V1	3.11	0.26	1.98	0.01	0.50	0.07	0.01	---	0.007	0.011	Bal.	320	260	765	800
V2	3.01	0.25	0.08	2.00	0.51	0.07	0.01	---	0.007	0.009	Bal.	340	260	780	820
A1	2.94	0.29	1.86	0.03	0.52	0.01	0.02	0.04	0.017	0.009	Bal.	330	220	750	780
A2	3.19	0.30	0.10	2.11	0.48	0.15	0.01	0.05	0.007	0.012	Bal.	320	195	750	780

*In V1 and V2, wt % of C is 0.22 and 0.24 respectively, in the bars from which tensile specimens were prepared.

V & A refer to vacuum and air melts respectively.

TABLE III TYPICAL ATOM PROBE ANALYSES OF CARBON CONCENTRATION IN MARTENSITE AND RETAINED AUSTENITE PHASES

	As-quenched	Tempered
Martensite	0.23 ± 0.08	0.07 ± 0.04
	0.31 ± 0.08	0.16 ± 0.05
	0.28 ± 0.13	
	0.14 ± 0.10	
Austenite	2 ± 0.68	2.25 ± 0.37
		2.27 ± 0.39
		2.64 ± 0.48

Figure Captions

1. Schematic showing the microduplex structure. Alloys are designed to produce dislocated lath martensite, surrounded by stable, thin films of retained austenite. Some autotempering may also occur as M_s is usually $\gtrsim$ 300°C.

2. (a) Bright field and (c) dark field TEM micrographs of Fe-3Cr-2Mn-0.3C-0.5Mo steel in the as-quenched condition revealing the general appearance of laths and retained austenite; (b) shows the indexed SAD pattern.

3. Mechanical properties summary showing toughness to strength relations in the experimental 0.3%C alloys and equivalent commercial alloys; (a) CVN impact energy vs. tensile strength.

4. (a) Bright field and (b) cementite dark field electron micrographs of specimens deformed in-situ in a 1 MeV microscope in the as-quenched and tempered martensite embrittled condition, respectively. Foils prepared from bulk aged samples. Note that the plastic zone evident in (a) is not present in (b); also, the crack is confined in the lath between the interlath carbides in (b) (see arrows). Figs. 4c and 4d are corresponding scanning fractographs taken from bulk Charpy specimens.

5. (a) Typical spectroscopic data obtained by field ion-atom probe taken from the martensite and retained austenite phases in tempered specimens; (b) distribution of carbon across the martensite/retained austenite interfaces in a 0.35%C steel, rapidly quenched ($10^3 ks^{-1}$).

6.(a) Distribution of carbon across the martensite/retained austenite interface in a 0.3%C steel tempered 1 h at 200°C showing unusually high peak, probably due to carbon build-up before carbide nucleation;(b) dark field TEM showing microstructure of alloy analysed in Fig. 6a after 200°C temper for 1 h (compare to Fig. 2); retained austenite is still present and Widmannstätten tempered interlath cementite is clearly resolved.

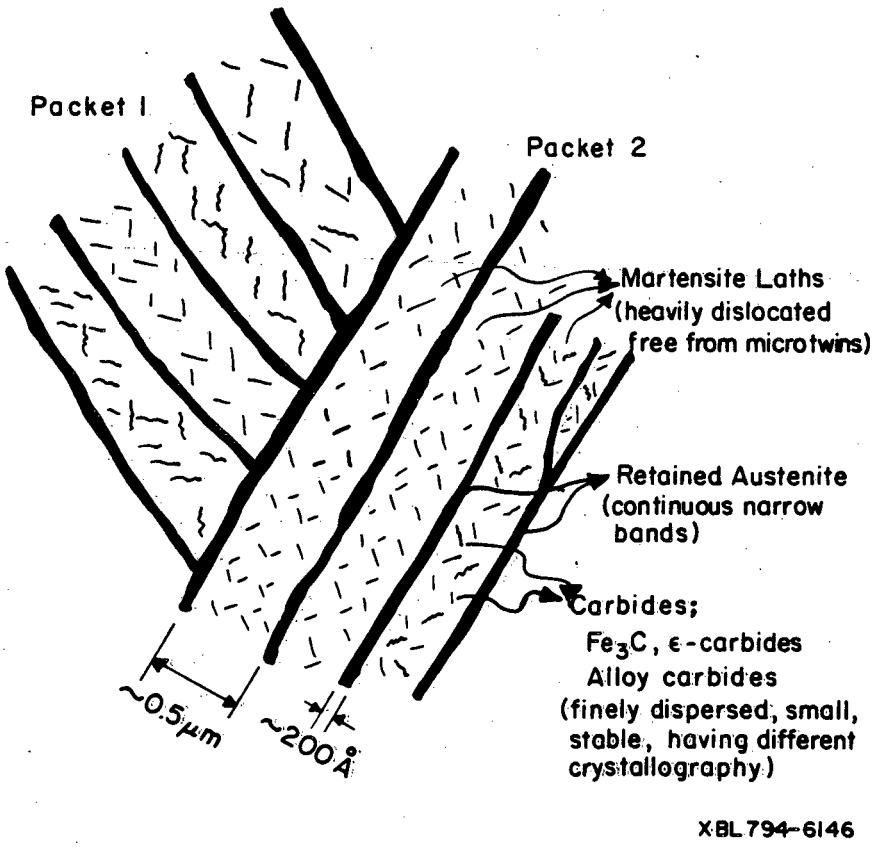
Packet 1
Packet 2
Martensite Laths
(heavily dislocated
free from microtwins)
Retained Austenite
(continuous narrow
bands)
Carbides;
Fe_3C, ε-carbides
Alloy carbides
(finely dispersed, small,
stable, having different
crystallography)
~0.5μm
~200Å
XBL794-6146

Fig. 1

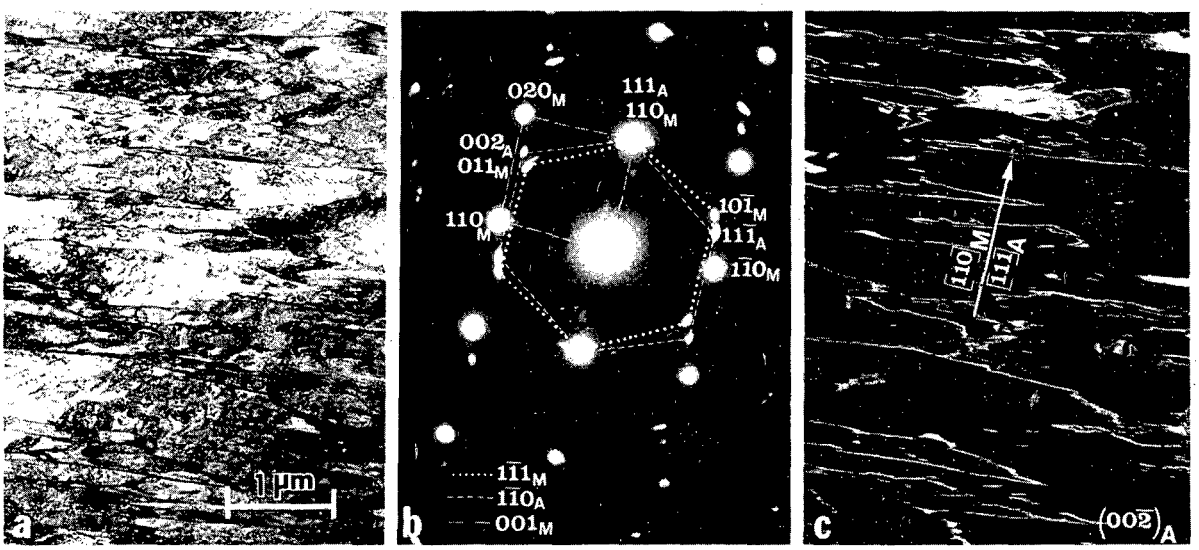

XBB-796 7880

Fig.2

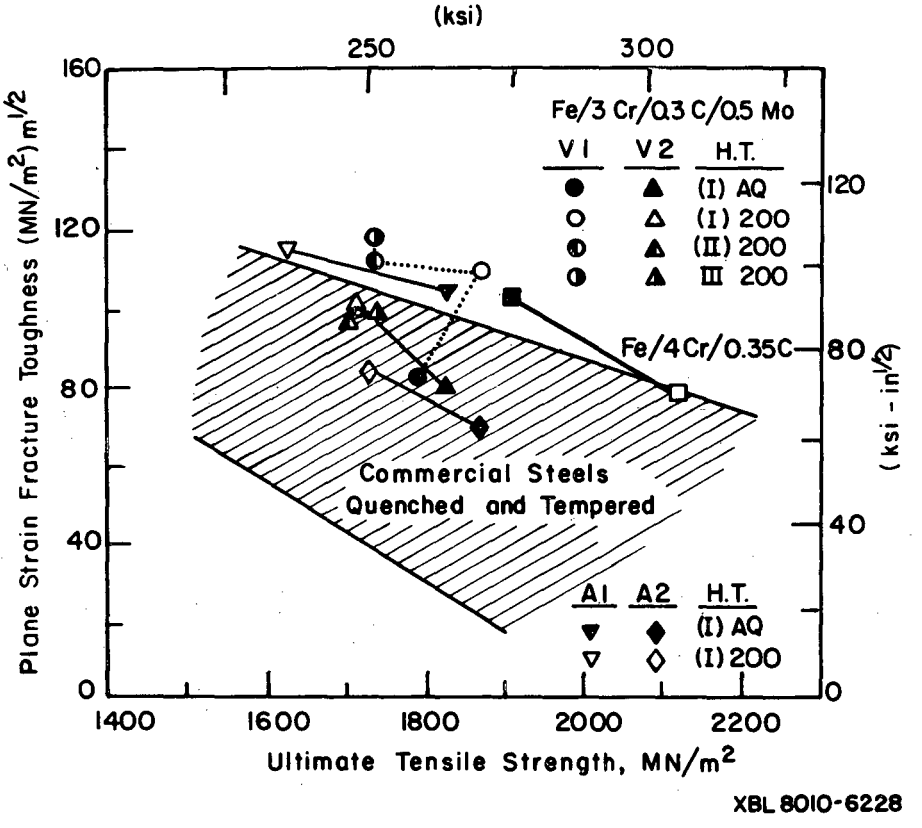
(ksi)
250
300
160
120
80
40
0
Plane Strain Fracture Toughness (MN/m²) m^1/2
Fe/3 Cr/0.3 C/0.5 Mo
V1 V2 H.T.
(I) AQ
(I) 200
(II) 200
III 200
Fe/4Cr/0.35C
Commercial Steels
Quenched and Tempered
A1 A2 H.T.
(I) AQ
(I) 200
120
80
40
0
(ksi - in^1/2)
1400
1600
1800
2000
2200
Ultimate Tensile Strength, MN/m²
XBL 8010-6228

Fig. 3-a

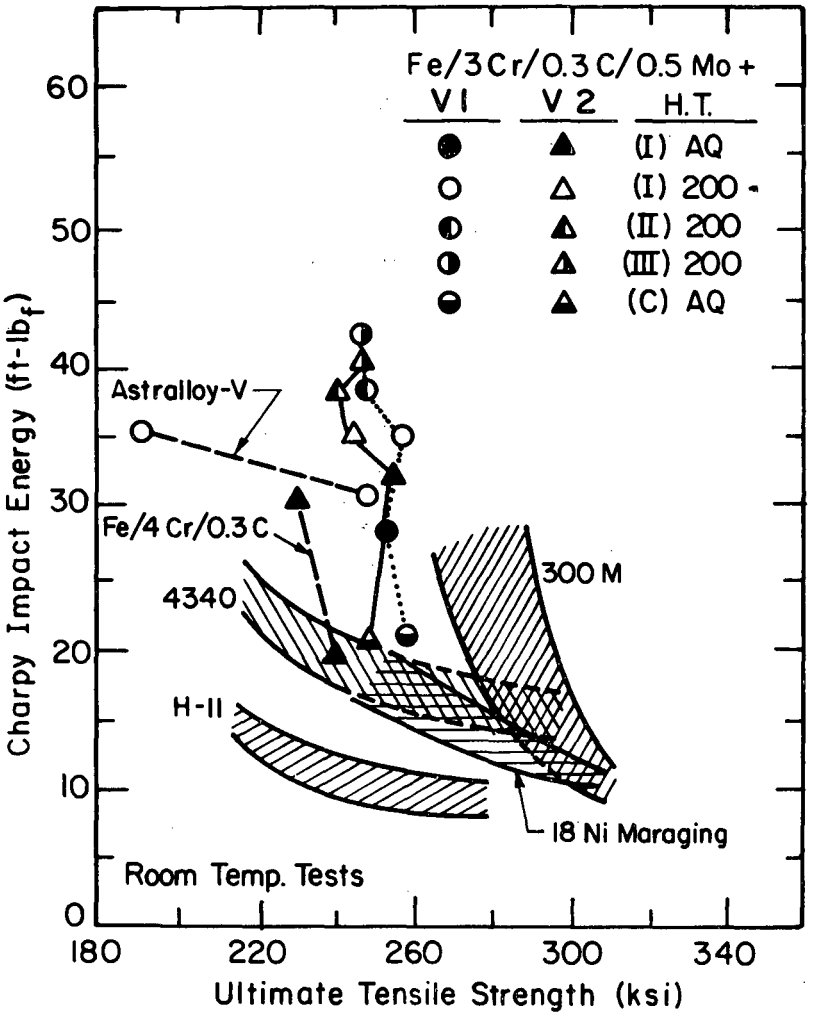

XBL 8010-6229

Fig. 3-b

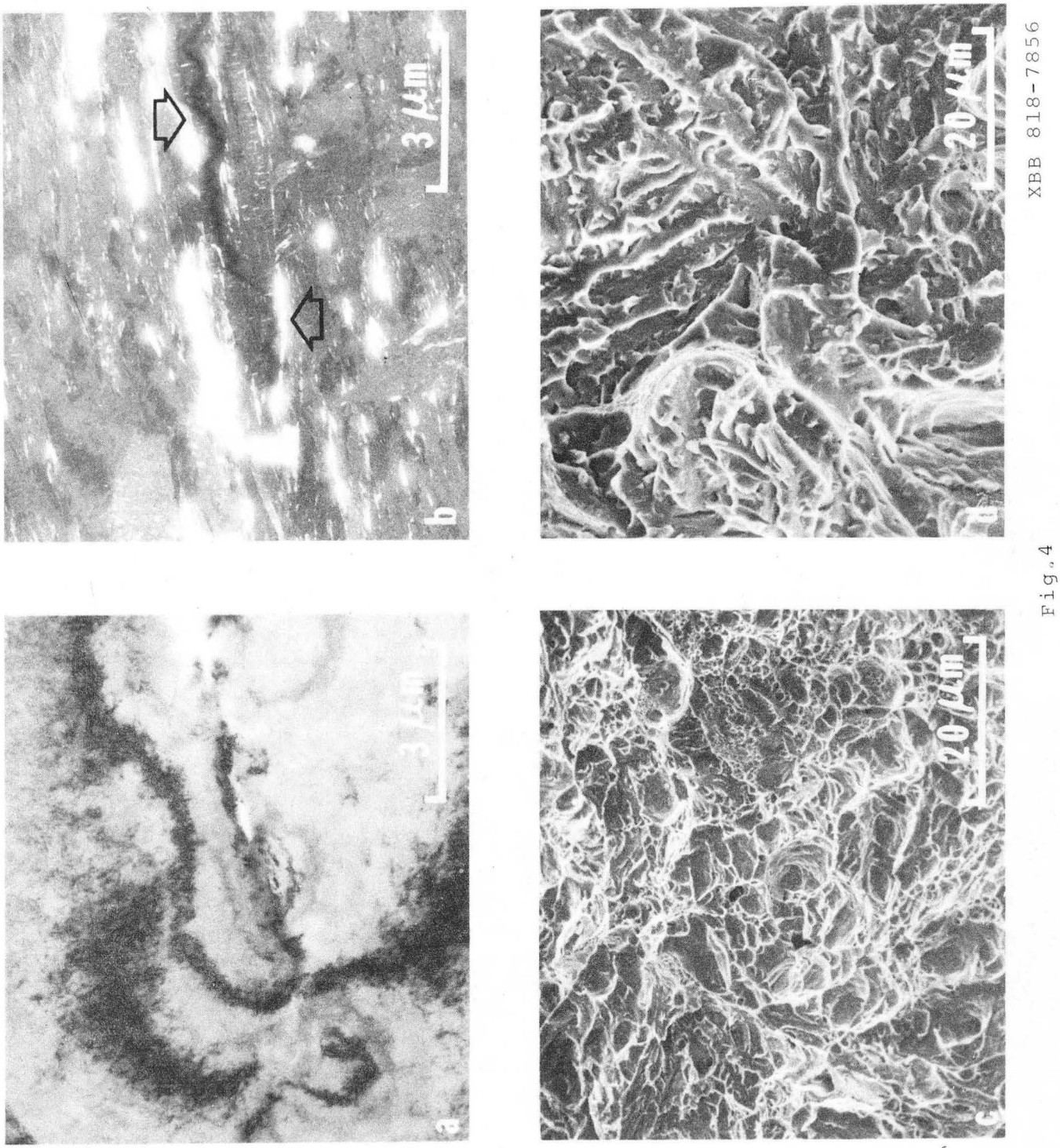

XBB 818-7856

Fig. 4

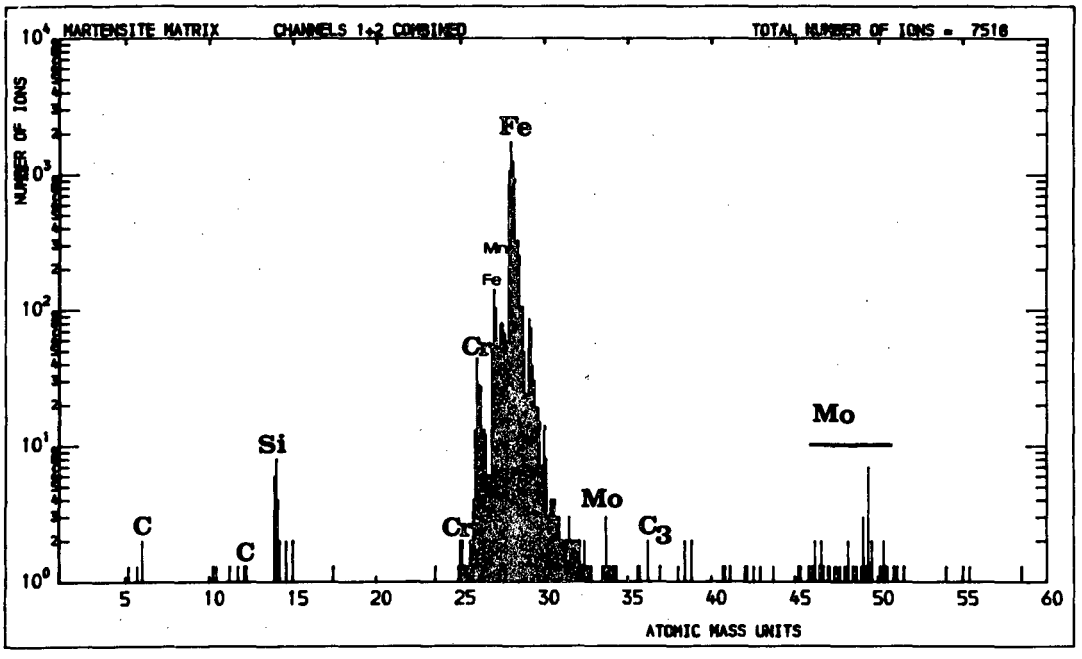

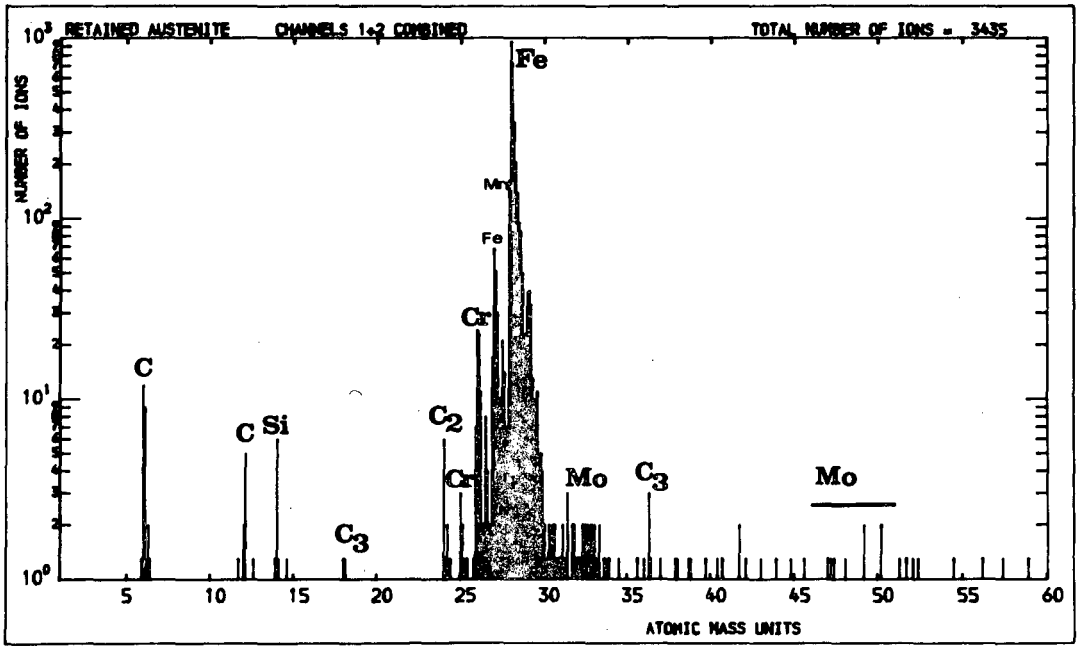

Fig.5-a

XBL 8112-12737

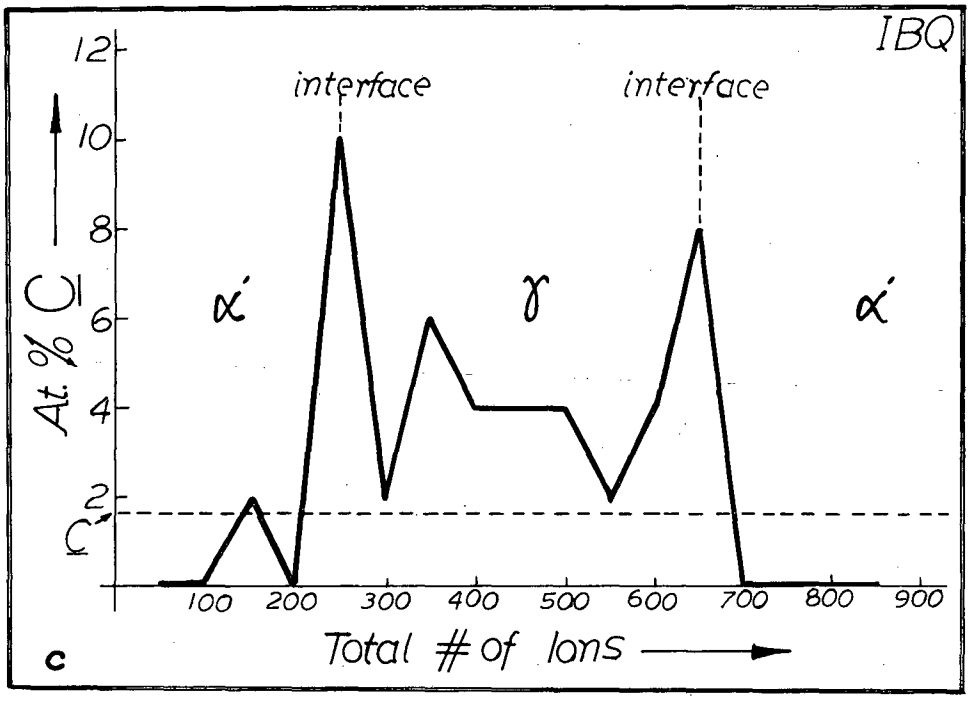

Fig. 5-b

XBB 821-1

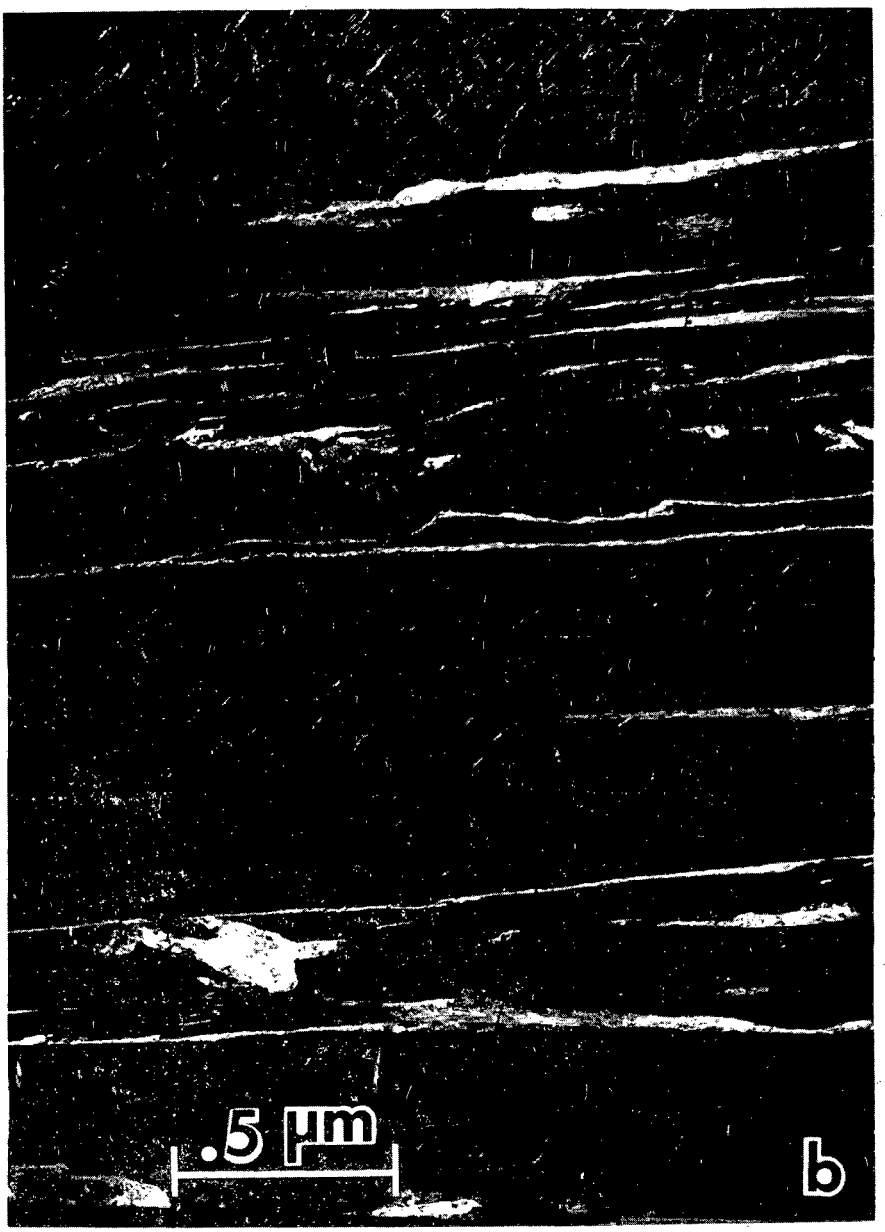

Fig.6-b XBB 794-4551

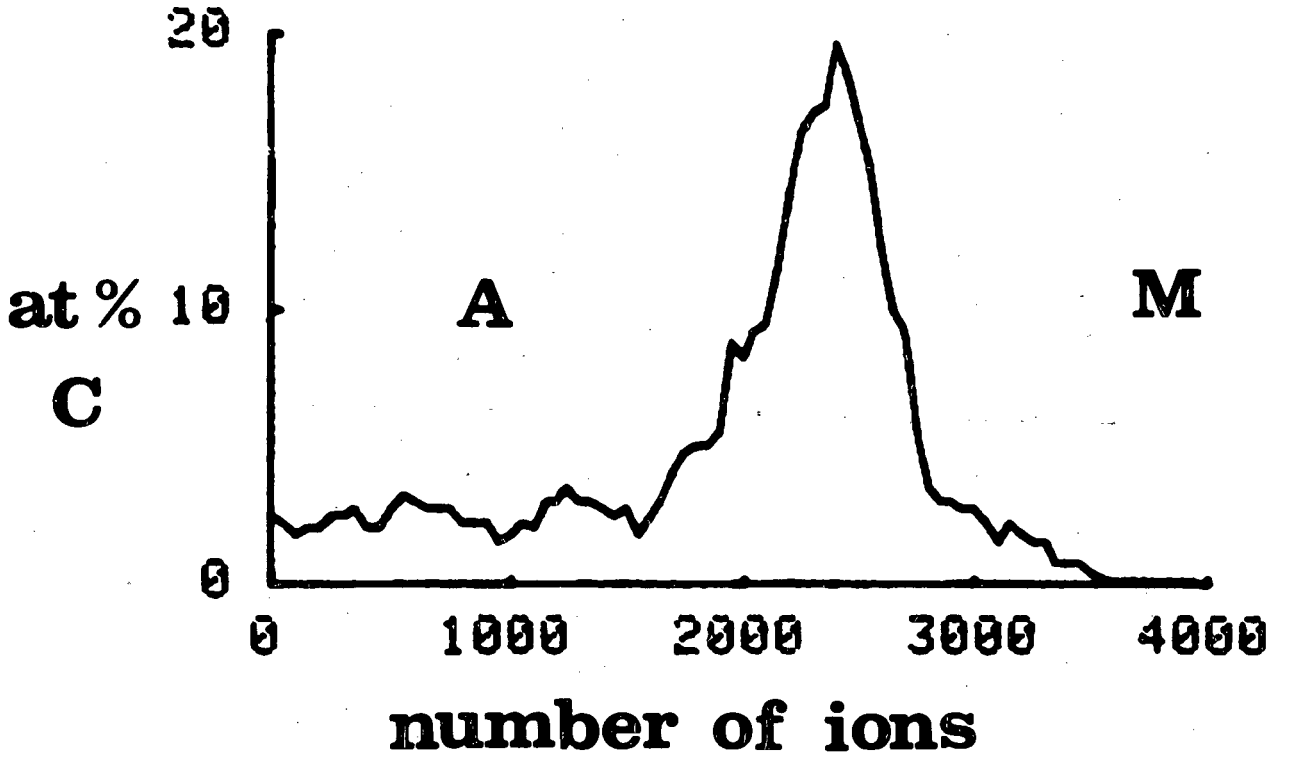

Fig.6-a

XBL 818-10981

This report was done with support from the Department of Energy. Any conclusions or opinions expressed in this report represent solely those of the author(s) and not necessarily those of The Regents of the University of California, the Lawrence Berkeley Laboratory or the Department of Energy.

Reference to a company or product name does not imply approval or recommendation of the product by the University of California or the U.S. Department of Energy to the exclusion of others that may be suitable.

TECHNICAL INFORMATION DEPARTMENT
LAWRENCE BERKELEY LABORATORY
UNIVERSITY OF CALIFORNIA
BERKELEY, CALIFORNIA 94720